Application of Interval and Depth Normalized Interval Velocities in the Determination of Gongola Basin Lithology for Hydrocarbon Exploration.

E.E.Epuh*, D. O.Olorode**, P. C. Nwilo* C. U. Ezeigbo*
* Department of Surveying and Geoinformatics, University of Lagos,
** Physics Department, University of Lagos.

ABSTRACT

The application of depth conversion using only the checkshot curve technique sometimes fail in areas of complex structures, tectonic inversion or lateral velocity change where insufficient well controls exist to adequately define the velocity variations in different lithologic units. In the Gongola Basin, the well information are sparse and the analysis of seismic reflection data had relied heavily on structural mode. This reliance on structural mode is necessary in view of the fact that seismic images of fold and thrust structures within the area are distorted and of uneven quality. Part of the strata geometry may be clearly shown while others show either a lack or a confusing surplus of reflection signals. Migrated results of uniform quality are difficult to obtain especially where seismic imaging is poor because of the complex structural geometry of the basin.

This article examines the application of depth normalized interval velocity computed using the integrated depth algorithm (IDA) iterative process to adequately address the depth conversion for the determination of the lithology of the basin. Seven horizons were highlighted for analysis and the interval and depth normalized interval velocities were produced to determine the lithology. The density, reflection coefficients and acoustic impedances of the horizons were also computed to determine the prospect.

Two leads were identified from the time/depth structural maps. The interval and depth normalized velocity maps generally followed the structural contours. This is due to the fact that depth of burial with compaction plays significant role in determining the velocity values. A gas prospect was found at the depth between 2100 and 2700m in the Kolmani River lead of the project area. The lead in the Garin Habin zone was found to be a result of velocity gradient and not hydrocarbon accumulation.

Key words: Interval, Depth normalized interval, velocity and lithology

INTRODUCTION

A time map may indicate a structural closure when in reality, there is a velocity gradient present and the true time structure is a dipping nose. Time data alone are also unreliable when a deep, steeply, sloping water bottom exists. In the above situation, velocity data provide the basis for seismic time-to-depth geological depth conversion techniques. They provide the basic lithology for prediction techniques. In areas where exploration objectives requires reliable depth conversion algorithm, two methods are commonly used: the layer cake and average velocity. In the former, the   values of interval velocity are obtained from well velocity survey, seismic times and

well depths, or seismic velocities. In the latter, average velocity values are usually derived from seismic velocity (Carter, 1993).

In this research, the interval and depth normalized interval velocities are used in lithology determination. In normalizing the interval velocity, our goal is to remove the effects of age and depth and leave only the effects of pore pressure and lithology (Carter and Siraki, 1993). In this, different normalized interval velocities reflect differences in lithology. The depth normalized velocity technique uses a layered earth model which has the advantage of allowing the average or interval velocity to vary. The velocities can vary upward or downward according to the behaviour of the time structure map. Once the interval velocity of a formation is transformed to a depth normalized interval velocity, the changes in value are due to lithology, not structure. The effects of structure have been removed through the normalization process. In this research, the Carter-Good iterative depth algorithm technique is utilized in the depth conversion. Fig 1 shows a layered earth model.
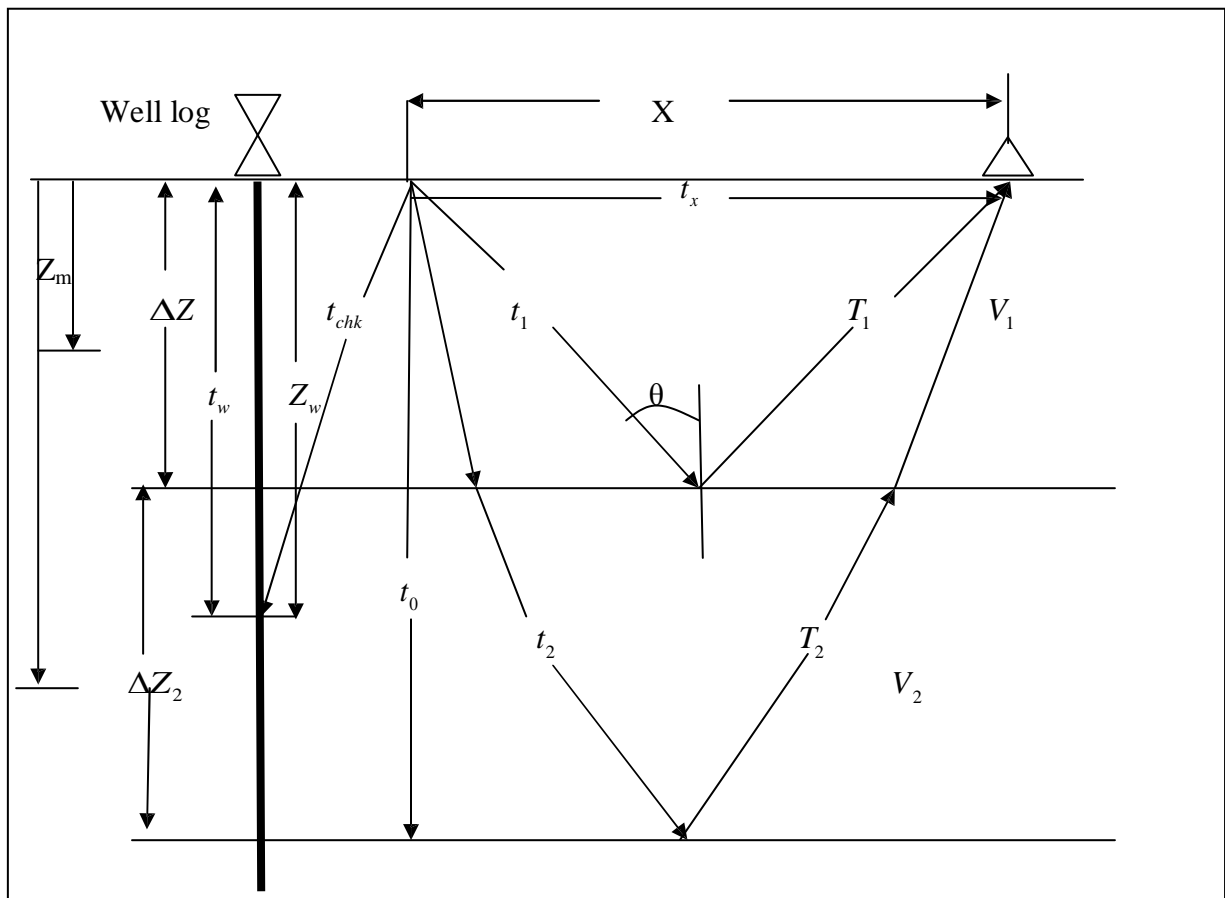

Fig.1: The Layered Earth Model (Source: Carter and Siraki, 1993)

From Fig 1.1, the following symbols are defined as follows:

t_{chk} = Traveltime recorded in a checkshot offset , T = two way travel time , t = one way travel time

t_w = travel time determined from well information , Z_w = depth measured from well information

$\theta =$ angle of incidence ,X=offset distance, $t_0 =$ Traveltime recorded at zero offset distance

2.0   Methodology

2.1   Data Capture

The structural data of the Gongola basin was carried out by identifying the units of similar reflection characteristics in the reflective sequence overlying the top basement. The time and depth data obtained from the seven horizons namely H_i (i=1, 6) and the top basement were used in the development of time and depth structural maps which were used for structural analysis of the basin. The identification of the reflection horizon was based on the continuity of the reflections and their relative amplitude using the opendtect workstation.

From the depth of each horizon obtained using the checkshot curve, the interval velocity was computed using equation 1.

$$V_i = 2(\frac{\Delta Z}{\Delta t})..1$$

V_i = interval velocity, $\Delta Z =$ thickness of layer $= Z_{n+1} - Z_n$

$\Delta t =$ vertical two way traveltime through layer $= t_{n+1} - t_n$

The interval velocity predicts the traveltime through an individual layer,

The depth normalized interval velocity is expressed as:

$$V_i' = V_i \left(\frac{Z_n}{Z_m}\right)^{1/N} ....2$$

$V_i' =$ normalized interval velocity, $V_i =$ interval velocity

$Z_n =$ the normalized depth, $Z_m =$ the midpoint depth, 1/N= compaction value

Utilizing the Carter-Good IDA technique, the following were carried out (Carter and Siraki, 1993):

1.   The datum is defined. In this research, the seismic reference datum (SRD) of 28.54m was given and this correlated to a seismic time of 30msec using the checkshot curve.

2.   The seismic reflection times for all the horizons of interest, including the datum surface, at every shot point is converted from time to depth.

3.   The normalized interval velocity is calculated. So, at every data point to be converted from time to depth, we have a seismic interval ΔT, a normalized interval velocity (V_i'), the compaction factor $(\frac{1}{N})$, the normalized depth (Z_N) and the datum (Z_l). These parameter are all given, our goal is to determine ΔZ.

Table 2.1 illustrates the computational process for the iterative depth algorithm. The parameters given are separated from the parameters to be determined.

Table 2.1: Iterative Depth Algorithm (IDA)

PARAMETERS GIVEN						PARAMETER TO BE DETERMINED				
T	ΔT	V_i'	1/N	Z_N	Z	Z	ΔZ	Z_M	V_i	$\Delta \hat{T}$
T_1										
	$\Delta T_{1.2}$	$V_{1.2'}$	$1/N_{1.2}$	$Z_{n1.2}$			$\Delta Z_{1.2}$	$Z_{1.2}$	$V_{1.2'}$	$\Delta \hat{T}_{1.2}$
T_2						Z_2				
	$\Delta T_{2,3}$	$V_{2,3'}$	$1/N_{2.3}$	$Z_{n2,3}$			$\Delta Z_{2.3}$	$Z_{2.3}$	$V_{1.2'}$	$\Delta \hat{T}_{2.3}$
T_3						Z_3				

(Source: Carter and Siraki, 1993)

By iterating between the estimates of the interval velocity and the interval time ΔT, the actual depth of the horizon can be determined. The values obtained from the iteration are used in the development of the depth map, interval velocity and normalized interval velocity maps for lithology determination. This method expresses the interval velocity in a format that allows smoothing and contouring of the control points without mimicking the structure or losing any structural information.

2.2 Interval Velocity Computations

The seven horizons picked for the time was correlated on the checkshot curve to produce their depth values. The interval velocity and normalized interval velocity data were computed using the iterative depth algorithm (IDA) procedure. The interval velocity of each horizon was computed using equation 1, while the normalized interval velocity was computed using equation 2. The interval velocity of horizon H1 was computed using the seismic reference datum (SRD) of 28.54m. This was correlated on the checkshot curve to give a seismic time of 30msec. They ΔT and Δ Z were obtained by subtracting the given SRD time (30msec) and depth (28.54m) from the horizon H1 time (T_1) and depth (Z_1) values. The normalized interval velocity was computed using a compaction factor of N=4.

2.3 Density Computation Using Gardner's Equation

Density is usually a function of velocity. By applying Gardner's equation (Dobrin and Savit,1988), density can be expressed as:

$$\rho = aV^{\frac{1}{4}} \dots\dots\dots\dots\dots\dots\dots\dots\dots\dots\dots\dots\dots\dots\dots\dots\dots\dots\dots\dots 3$$

*where* ρ is given in g/cm^3 and *V* in m/s when *a*=0.31 and in ft/s when *a*=0.23

3.0   Results and Analysis

3.1   Velocity Model Results

The seven horizons picked for the time and depth structure maps were also analyzed by developing the interval velocity and depth normalized interval velocity maps using the iterative depth algorithm (IDA) procedure. Table 3.1 gives the various results obtained for each horizon. Fig. 3.1 and 3.2 show the time and depth structure maps, while Fig 3.3 and 3.4 show the interval and depth normalized interval velocity of the prospect horizon.

Table 3.1: Summary of Structural, Velocity and Lithology Results

Horizon	Depth (m)	Structural Lead		Interval Velocity x1000 (m/s)		Normalized Interval Velocity x1000 (m/s)		Density (gcc)		Reflection Coefficient		Acoustic Impedance X1000		Lithology	
		Time	Depth	L-A	L-B	L-A	L-B	L-A	L-B	L-A	L-B	L-A	L-B	L-A	L-B
H1	0-500	NIL	NIL	2.70	2.80	2.81	2.91	2.23	2.26	1.00	1.00	6.03	6.31	Shale	Shale
H2	500-1500	NIL	NIL	2.70	3.10	2.81	3.22	2.23	2.31	0.00	0.06	6.03	7.17	Shale	Shale
H3	1500-2100	NIL	NIL	2.70	3.30	2.81	3.43	2.23	2.35	0.00	0.04	6.03	7.75	Shale	Shale
H4	2100-2700	L-A/L-B	L-A/L-B	2.75	3.20	2.86	3.33	2.24	2.33	0.01	-0.02	6.17	7.46	Shale	Gas sand
H5	2700-3900	L-A/L-B	L-A/L-B	2.80	4.96	2.91	5.16	2.26	2.60	0.01	0.27	6.31	12.90	Shale	Water Sand
H6	3900-5200	L-A/L-B	L-A/L-B	4.45	5.58	4.62	5.80	2.53	2.68	0.28	0.07	11.27	14.95	Dolo-mite	Dolo-mite
Base-ment	5200	NIL	NIL	4.50	6.20	4.68	6.45	2.54	2.75	0.01	0.07	11.43	17.05	Dolo-mite	Gneiss
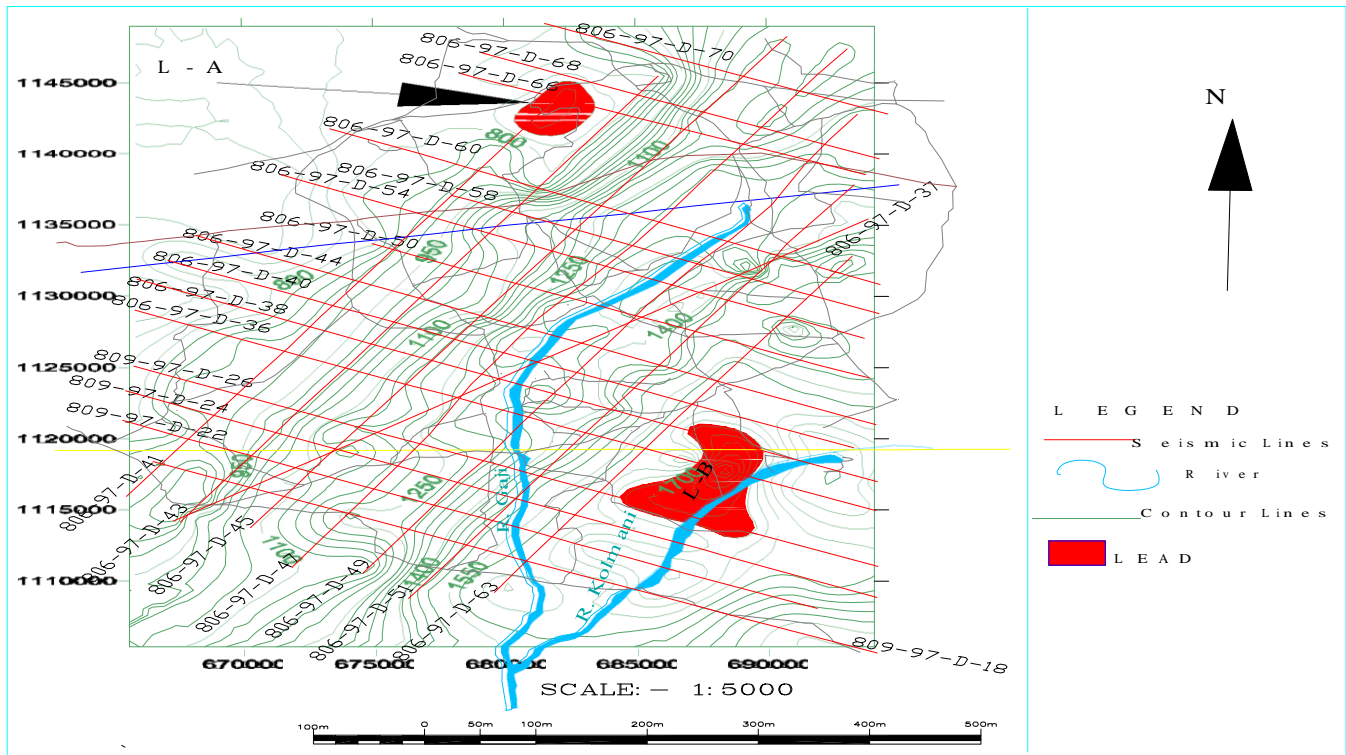
Fig. 3.1: Horizon H4 Time Structure Map (Contour interval =50msec)
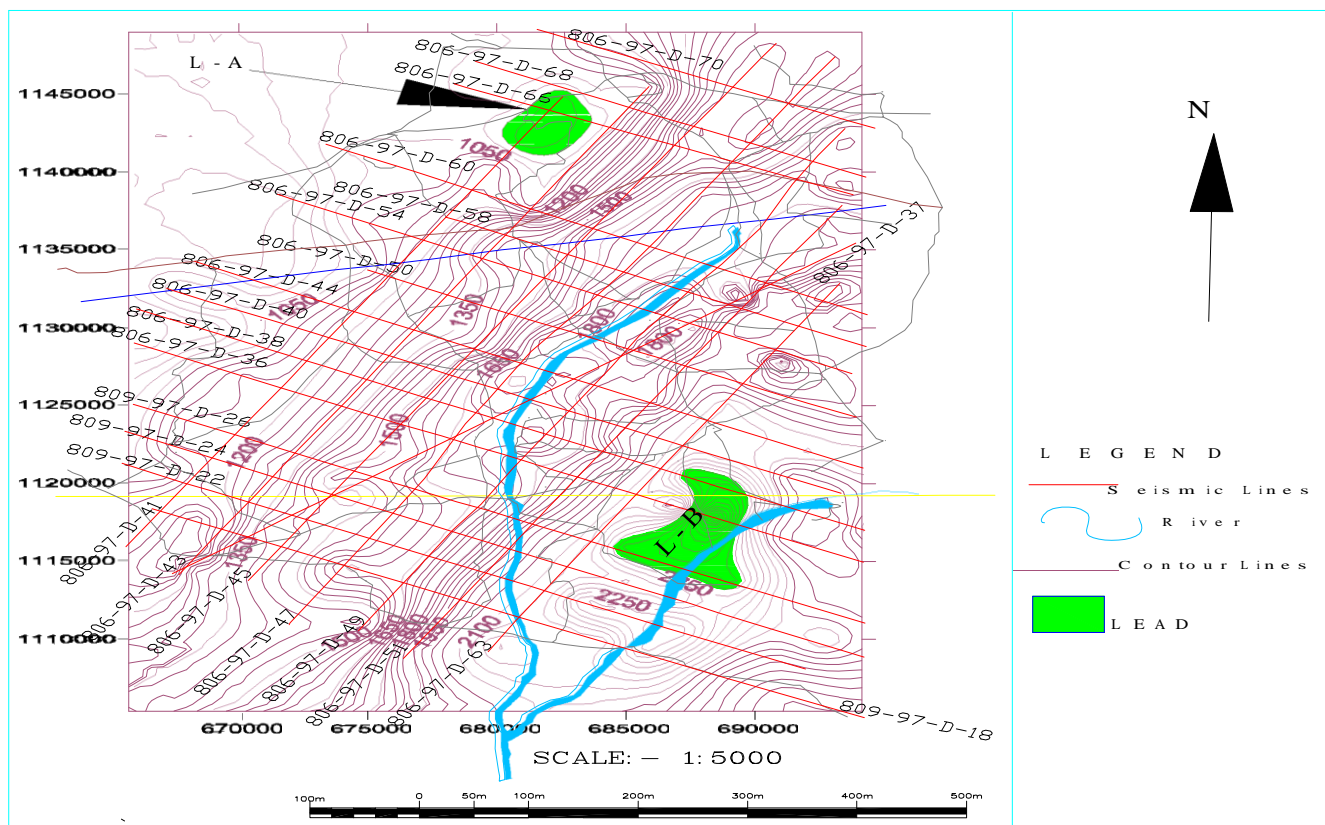
Fig 3.2: Horizon H4 Depth Structure Map (Contour Interval =50m)

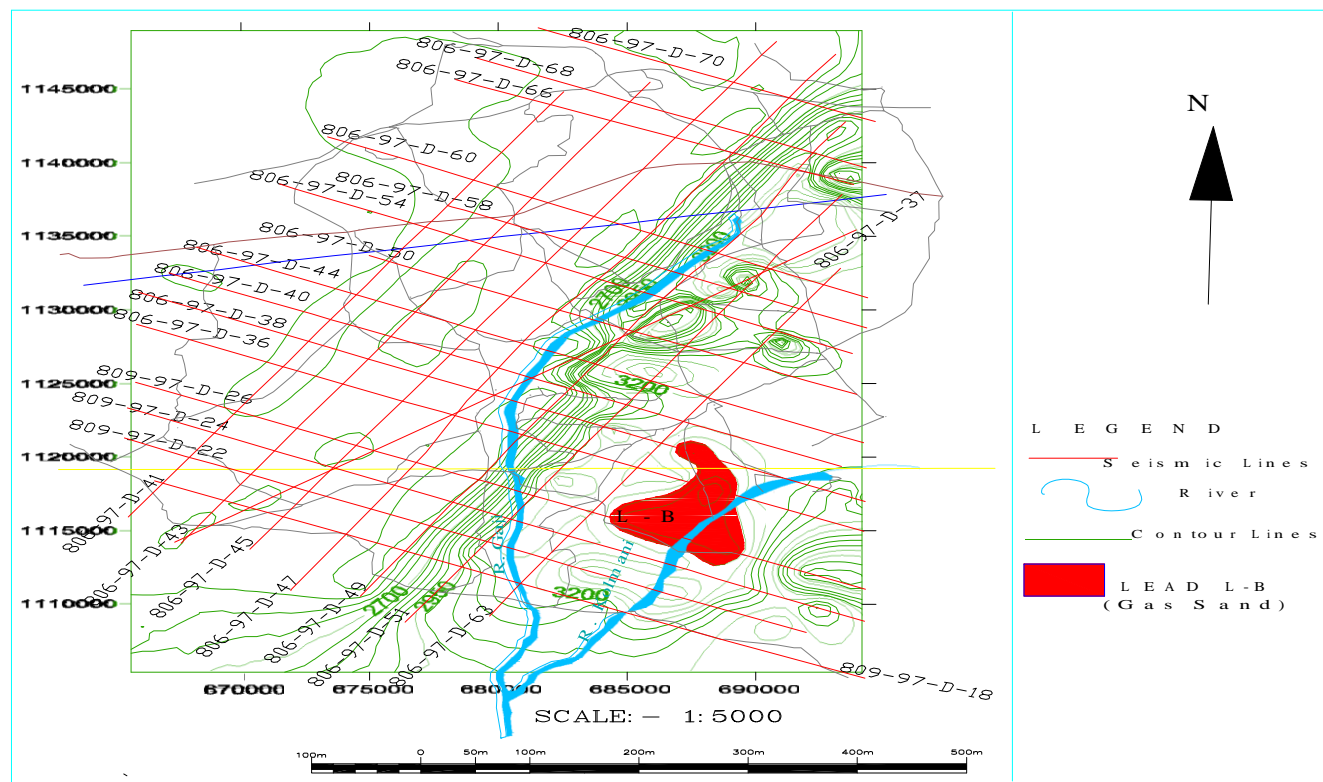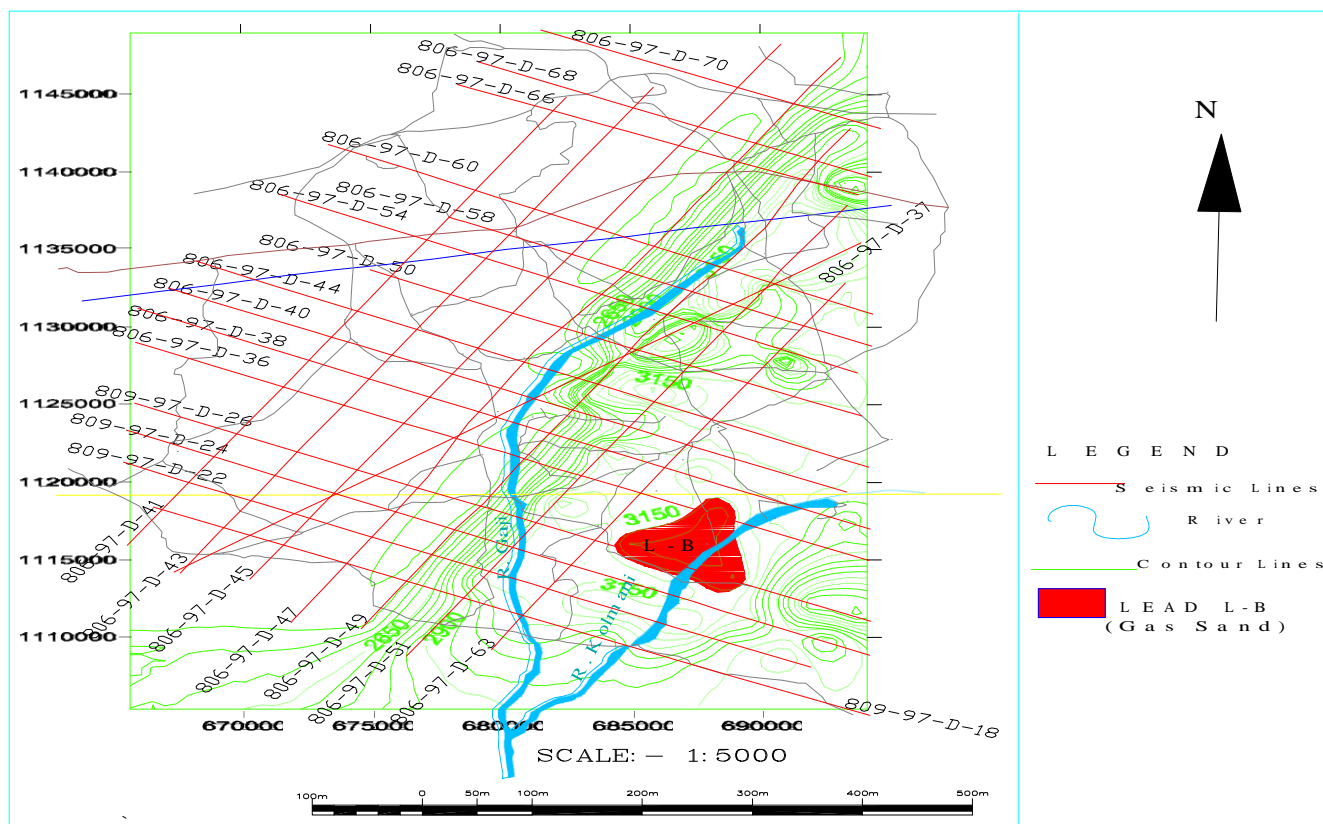**Fig 3.3: Horizon H4 Interval Velocity Map (contour interval =50m/s)**

Fig 3.4: Horizon H4 Normalized Interval Velocity Map (contour interval =50m/s)

3.2   Time/Depth Structure Map Analysis

From the time/depth structure maps of horizon H4 in Fig 3.1 and 3.2, two lead locations: L-A in Garin Habin and L-B in Kolmani River were identified on the maps. The leads were also identified in horizons H5 and H6 in the time/depth structure maps. These lead locations could not be traced in horizons H1, H2 and H3 in the time/depth structure maps.

3.3   Velocity Map Analysis

Below is the analysis of the interval and depth normalized interval velocity maps of each horizon.

i.   Horizon H1

This is the shallowest horizon of all the horizons. The lateral velocity variation is not significant across the entire basin. The resulting lateral velocity variation is due to the effect of geomorphology at the surface. The interval velocity of this horizon varies from 2700m/s in lead L-A to 2800m/sin lead L-B, while the normalized interval velocity varies from 2810m/s in lead L-A to 2910m/s in lead L-B respectively. The lithology identified at this horizon is sandstone and shale. The interval and depth normalized interval velocity maps are shown in Appendix A (A1 and A7)

ii.   Horizon H2

There was no significant lateral velocity variation at this horizon across the basin. This is due to a unified sediment compaction at this horizon. The interval velocity of this horizon varies from 2700m/s in lead L-A to 3100m/sin lead L-B, while the normalized interval velocity varies from 2810m/s in lead L-A to 3220m/s in lead L-B respectively. The lithology is identified as dolomite and shale. The interval and depth normalized interval velocity maps are shown in Appendix A(A2 and A8)

iii.   Horizon H3

The lateral velocity variation in this basin has started becoming prominent at this horizon. This is due to differential sedimentation and subsidence. The interval velocity of this horizon varies from 2700m/s in lead L-A to 3300m/sin lead L-B, while the normalized interval velocity varies from 2810m/s in lead L-A to 3430m/s in lead L-B respectively. The horizon shows that the dominant lithology is shale. The interval and depth normalized interval velocity maps are shown in Appendix A(A3 and A9)

iv.   Horizon 4

The lateral velocity variation becomes much more prominent at this horizon displaying its significance between inline 806-97-D-63 and 806-97-D-49 and prograding upward. The prominence of the variation is shown in the lead L-B loop closure exhibiting correlation of lithology within the lead. The lead L-A closure is not affected by the prograding of the sediments. The reflection coefficient is 0.01 in L-A and -0.02 in L-B, suggesting that the loop closure in L-B does contain a gas prospect. The interval velocity of this horizon varies from 2750m/s in lead L-A to 3200m/sin lead L-B, while the normalized interval velocity varies from 2860m/s in lead L-A to 3330m/s in lead L-B respectively. The lithology is identified

as dolomite and shale (Gas Sand). The interval velocity and depth normalized interval velocity maps of horizon H4 are shown in appendixes Fig 3.3 and 3.4 respectively.

v.   Horizon H5

At this horizon, the lateral velocity variation becomes more prominent; defining more realistically, the prospect loops closure at L-A and L-B. The variations extend to inline 806-97-D-45. The interval velocity of this horizon varies from 2700m/s in lead L-A to 4960m/sin lead L-B, while the normalized interval velocity varies from 2910m/s in lead L-A to 5160m/s in lead L-B respectively.   The lithology is identified as dolomite and shale (water sand). The interval and depth normalized interval velocity maps are shown in Appendix A(A4 and A10)

vi.   Horizon H6

At this horizon, the lateral velocity variation has become erratic extending to the inline   806-97-D- 41. The leads are still defined as in time and depth structure maps extending its area coverage. The interval velocity of this horizon varies from 4450m/s in lead L-A to 5500m/s in lead L-B, while the normalized interval velocity varies from 4620m/s in lead L-A to 5800m/s in lead L-B respectively.. The lithology is identified as Dolomite and shale. The interval and depth normalized interval velocity maps are shown in Appendix A (A5 and A11)

vii.   Top Basement.

At this horizon the lateral velocity variation becomes even more erratic. The interval velocity of this horizon varies from 4500m/s in lead L-A to 6200m/sin lead L-B, while the normalized interval velocity varies from 4680m/s in lead L-A to 6450m/s in lead L-B respectively. The interval and depth normalized interval velocity maps are shown in Appendix A (A6 and A12)

3.3   Summary of Findings

i.   The interval velocity maps generally followed the structural contours. This is due to the fact that depth of burial with compaction plays significant role in determining the velocity values.

ii.   The changes obtained in the maps are related to changes in lithology, porosity and depth.

iii.   The reflection coefficients in horizon H4 (L-B) show that the prospect is gas.

iv.   The structural closure in lead L-A is found to be a result of velocity gradient rather than hydrocarbon accumulation.

4.0   Conclusion

The interval and depth normalized interval velocities computed using the integrated depth algorithm (IDA) correlated with the geology of the basin and a gas prospect was discovered. When converting time to depth in seismic model, both well data and seismic data are required. Well data provide the calibration but lack the sampling density required when the velocity gradients and lithologic variations exist. A seismic survey has the
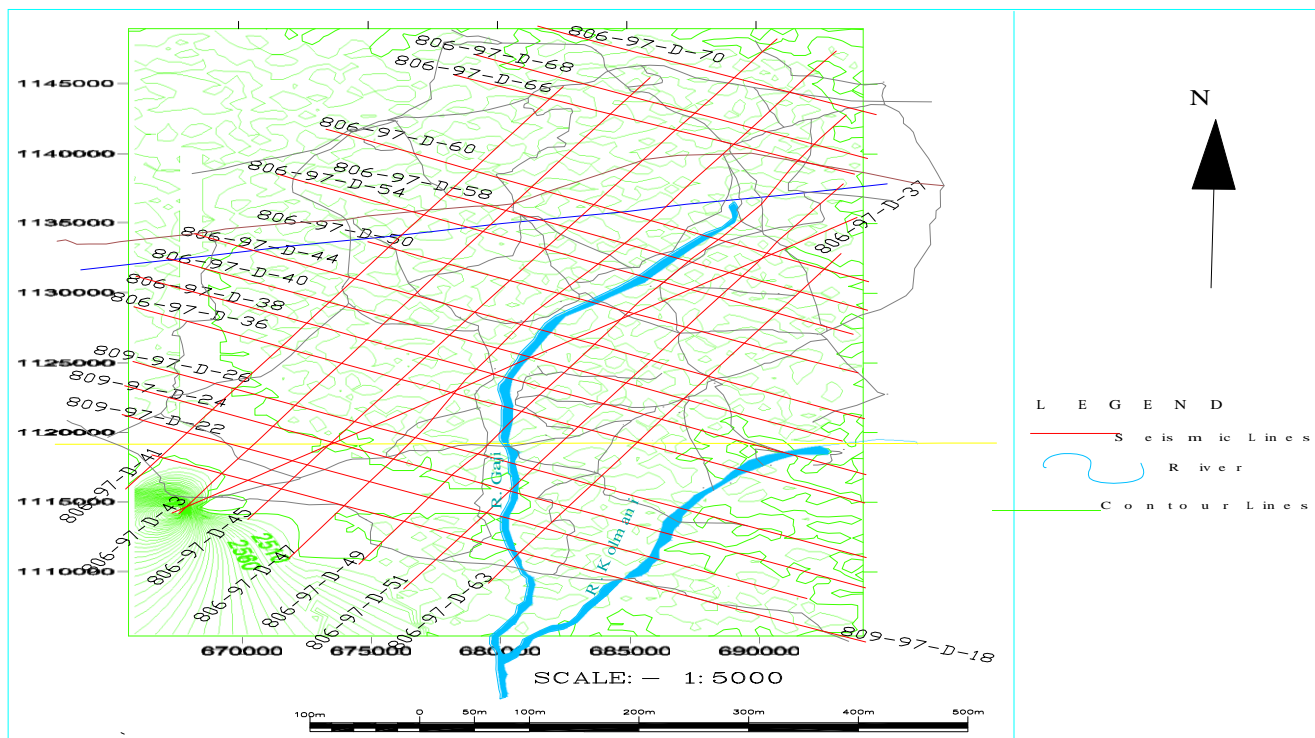
sampling density but cannot be used alone in depth calibration. When the two datasets are integrated, they provide a better depth and lithology definitions within a basin.
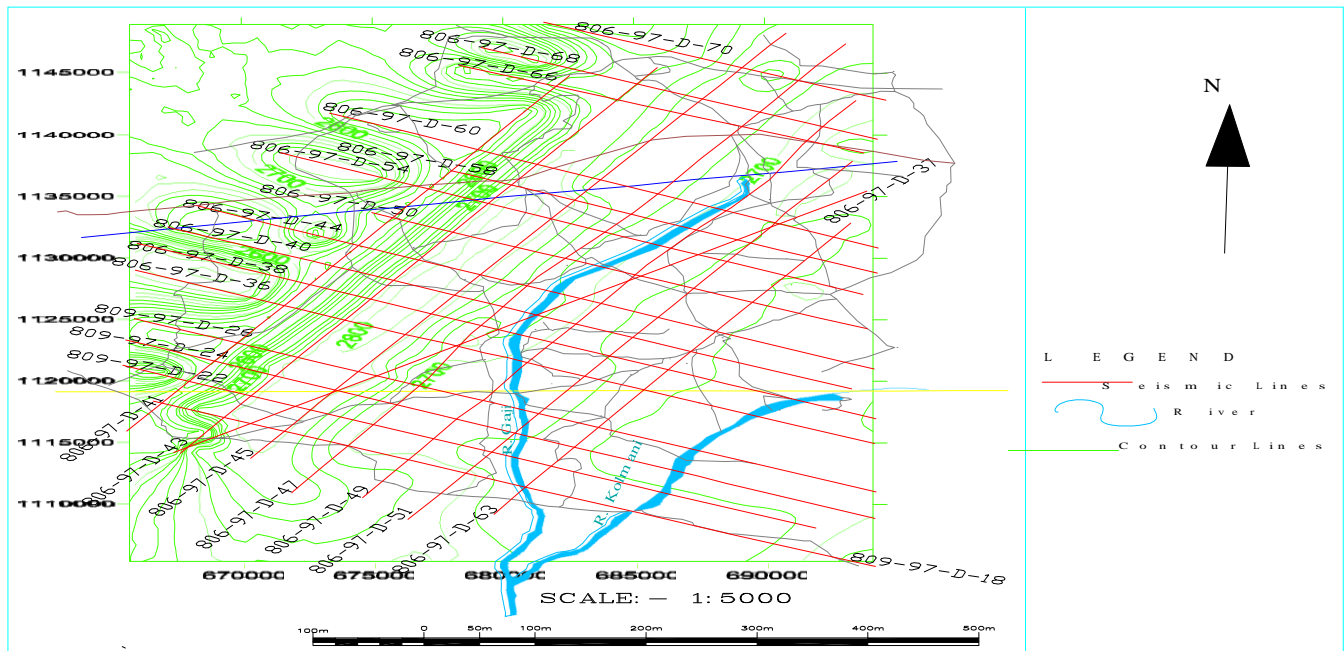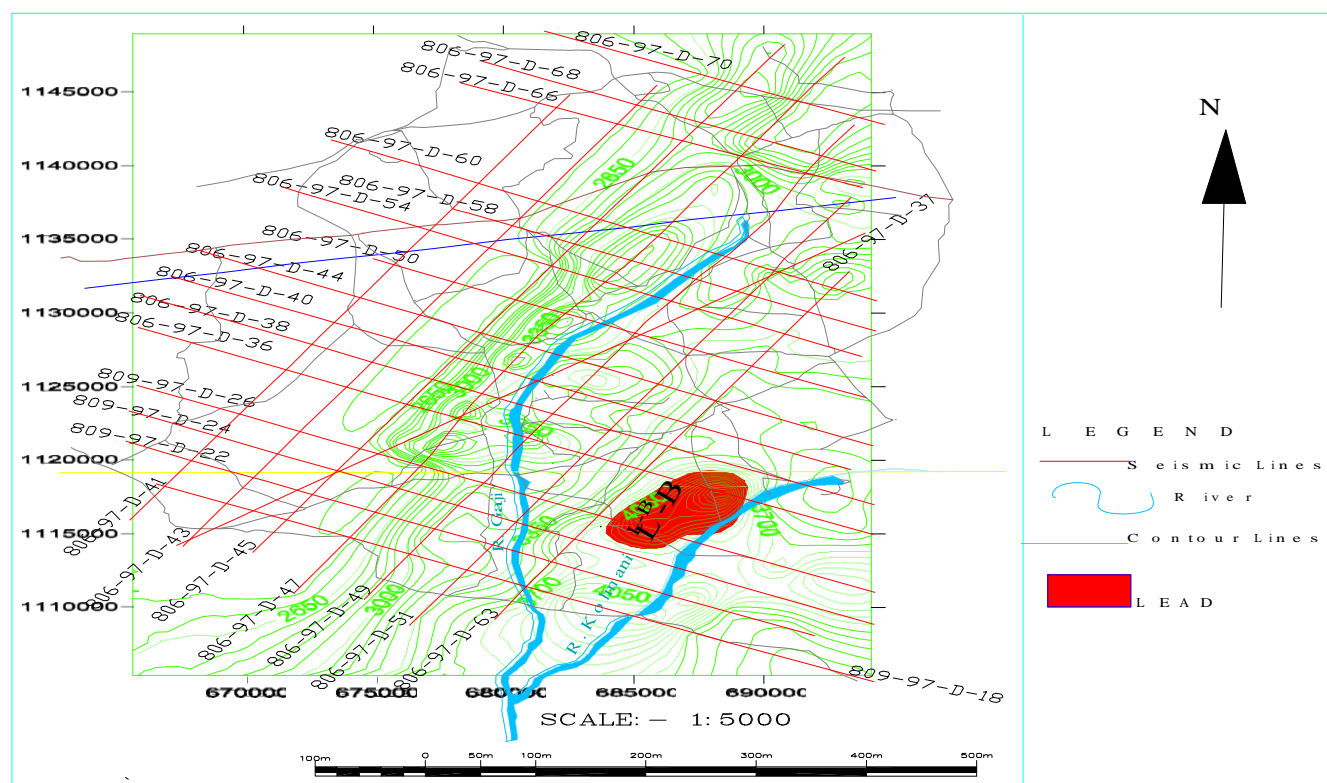

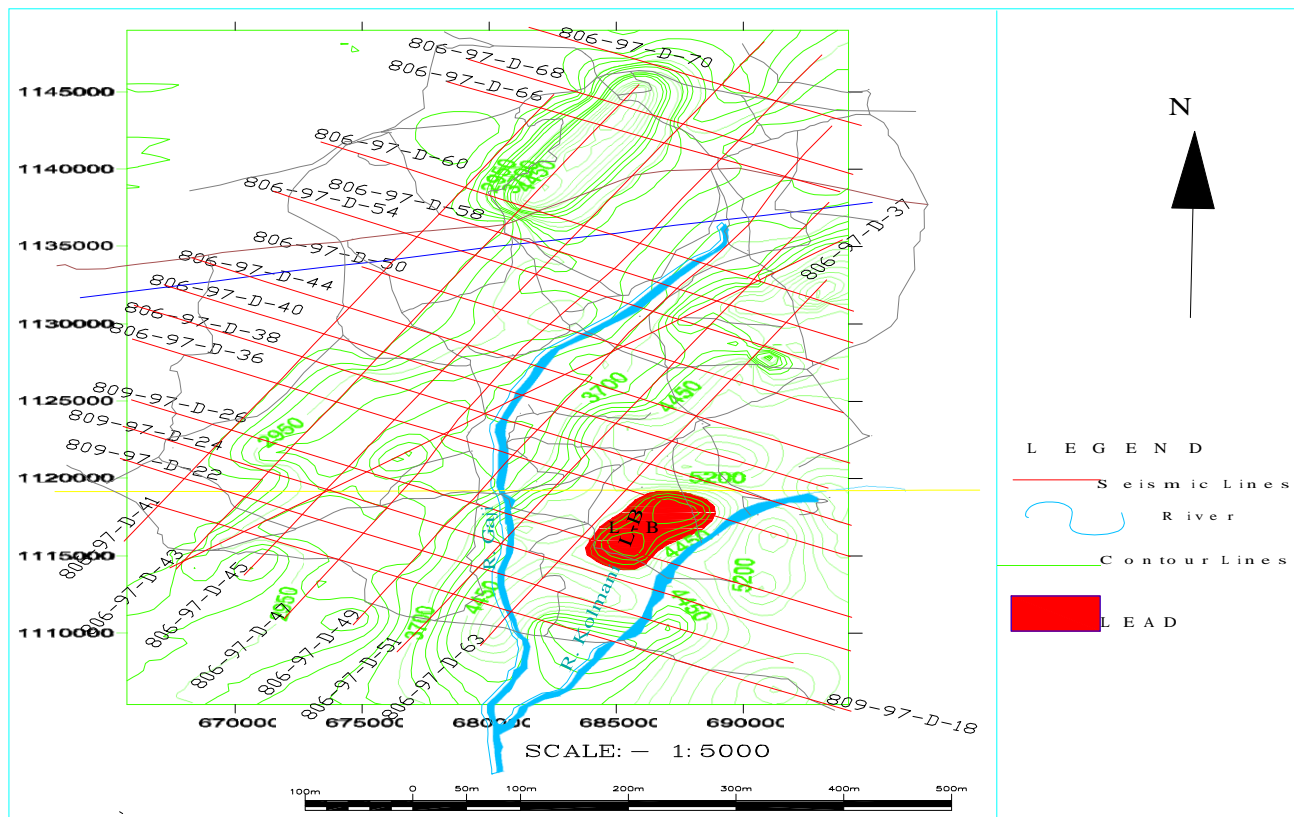**A1: Horizon H1 Interval Velocity Map (contour interval =50m/s)**
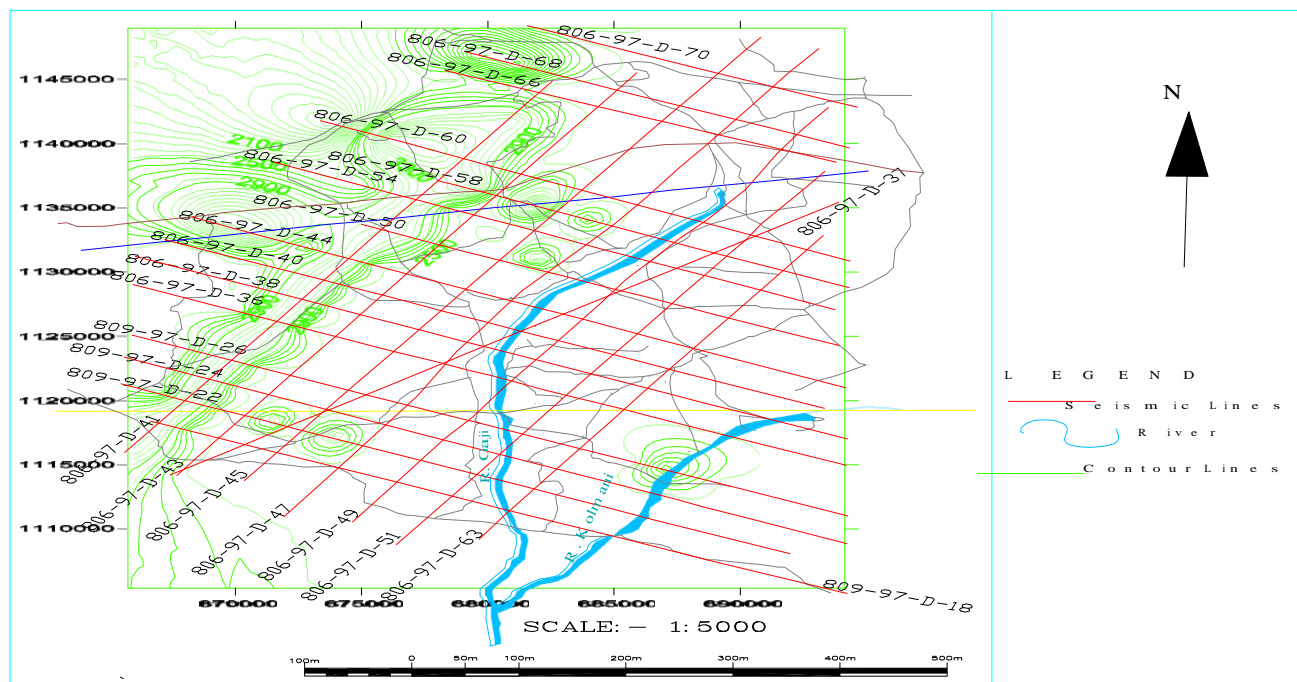
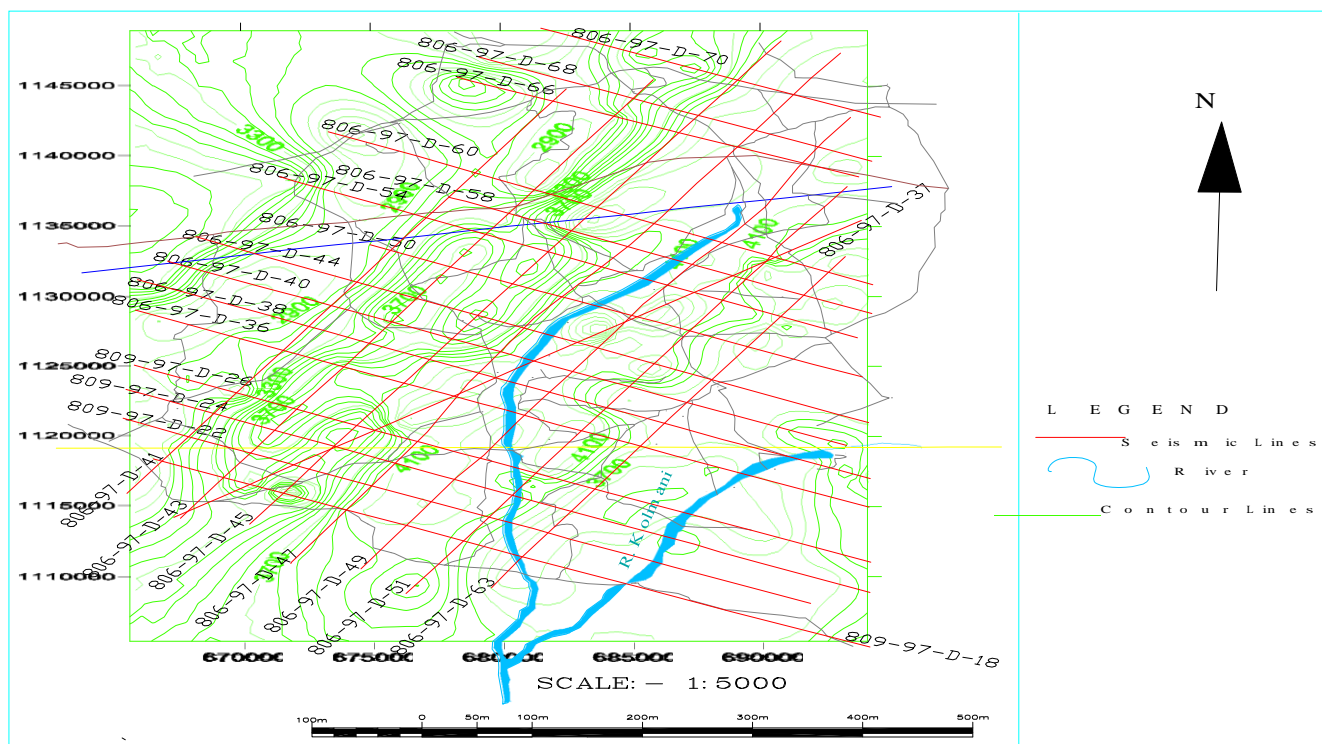**A2: Horizon H2 Interval Velocity Map (contour interval =50m/s)**

A3: Horizon H3 Interval Velocity Map (contour interval =50m/s)

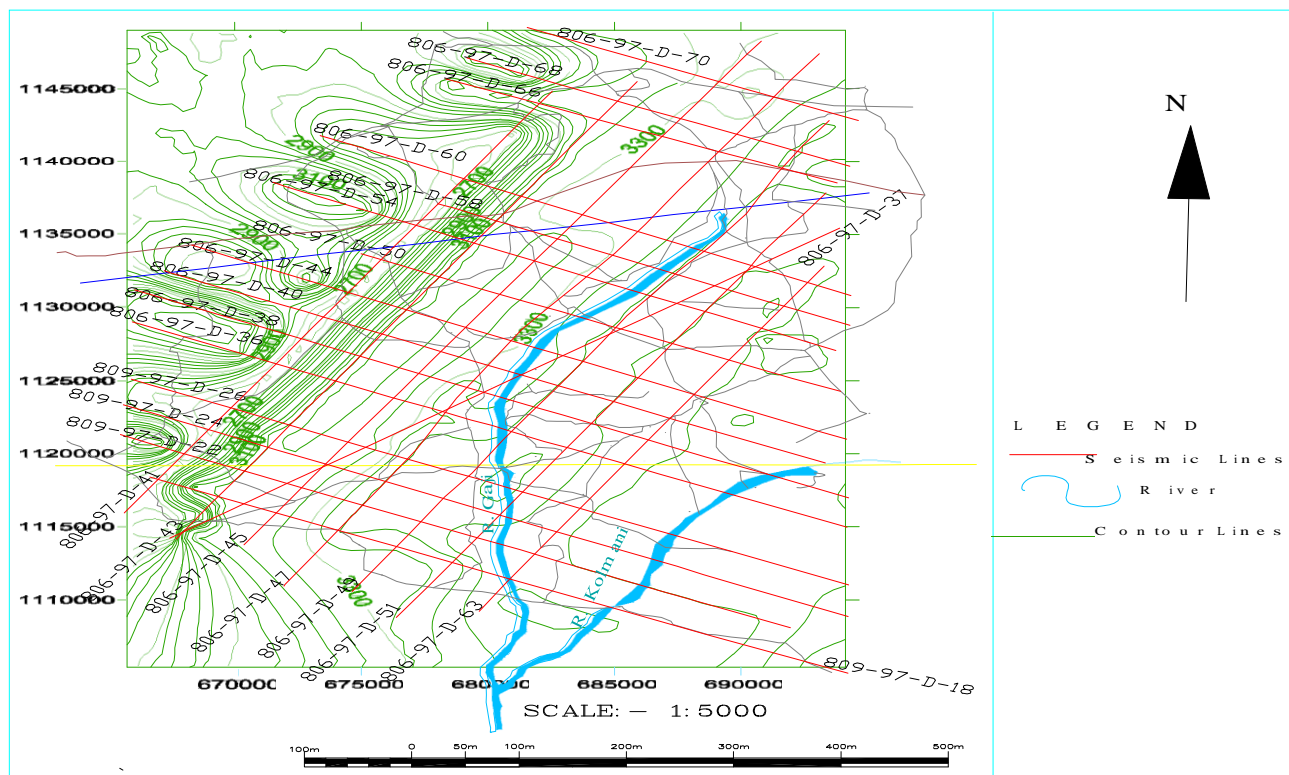**A4: Horizon H5 Interval Velocity Map (contour interval =50m/s)**

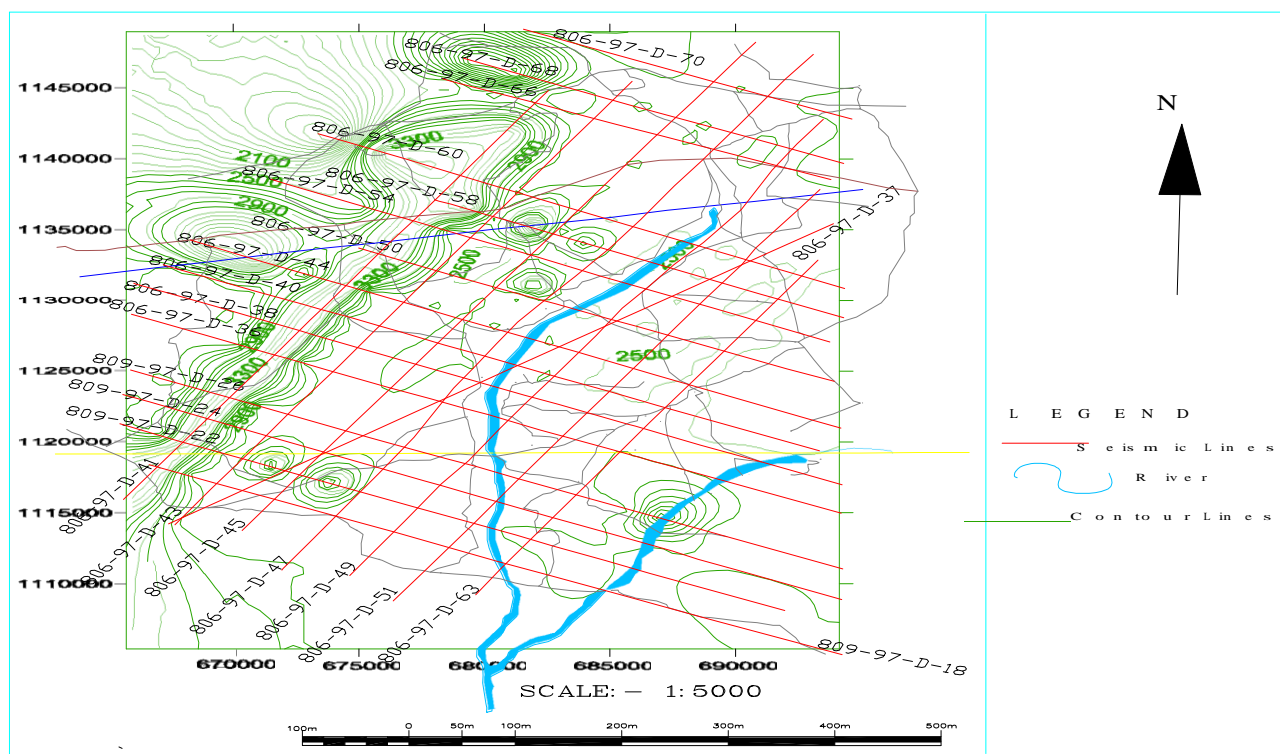A5: **Horizon H6 Interval Velocity Map (contour interval =50m/s)**

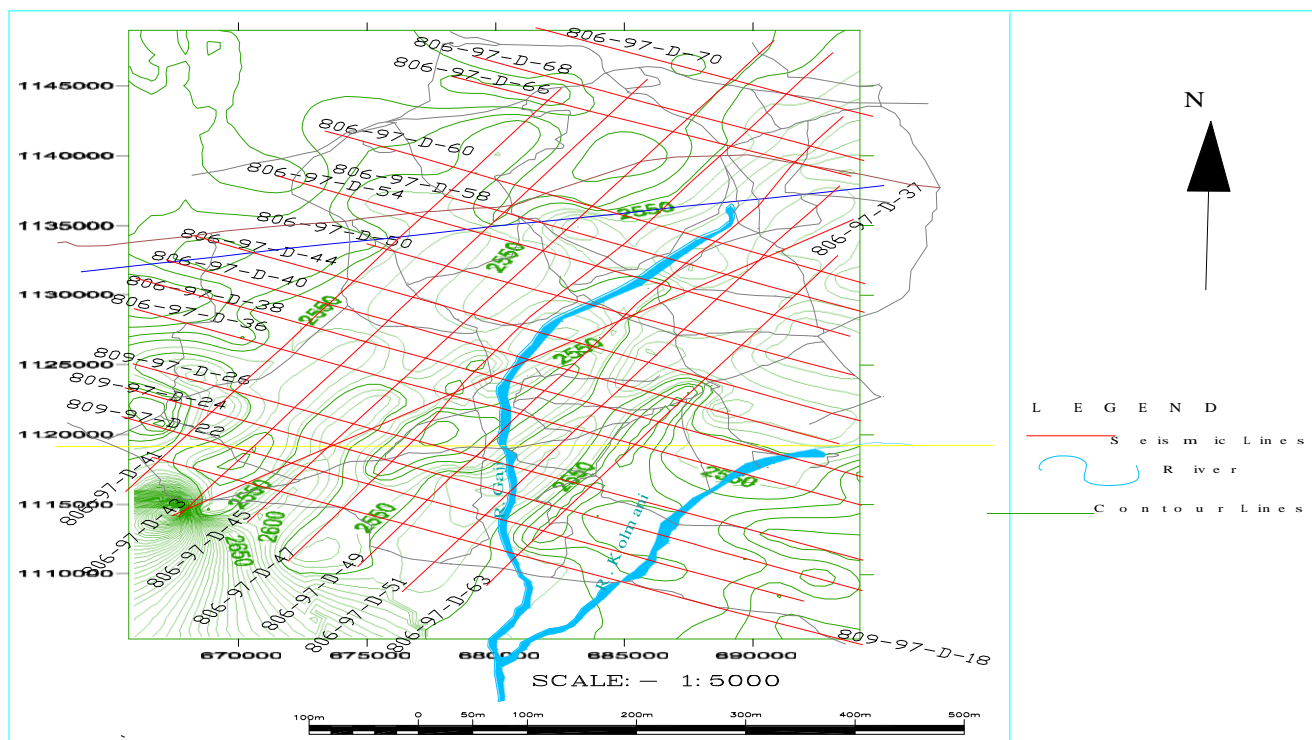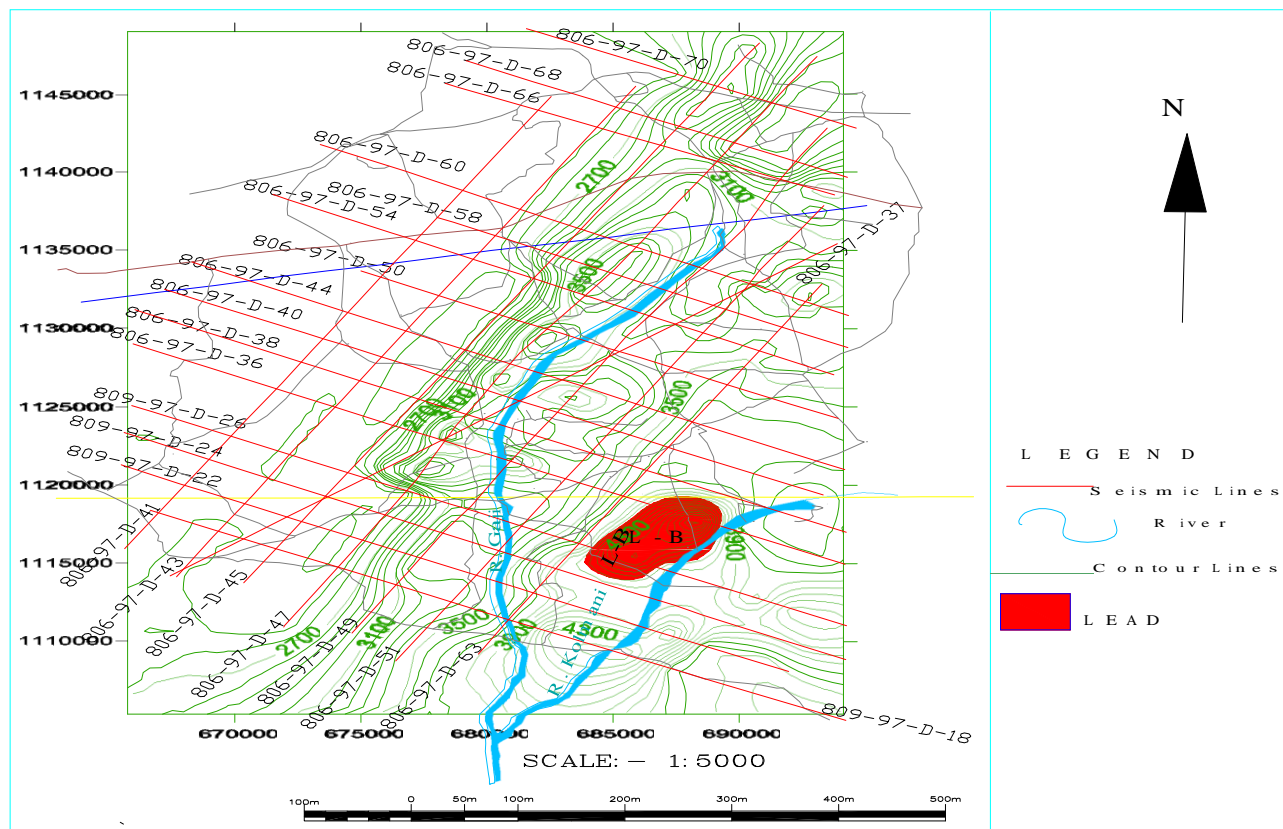**A6: Top Basement Interval Velocity map (contour interval =50m/s)**

A7**: Horizon H1 Depth Normalized Interval Velocity Map (contour interval =50m/s)**

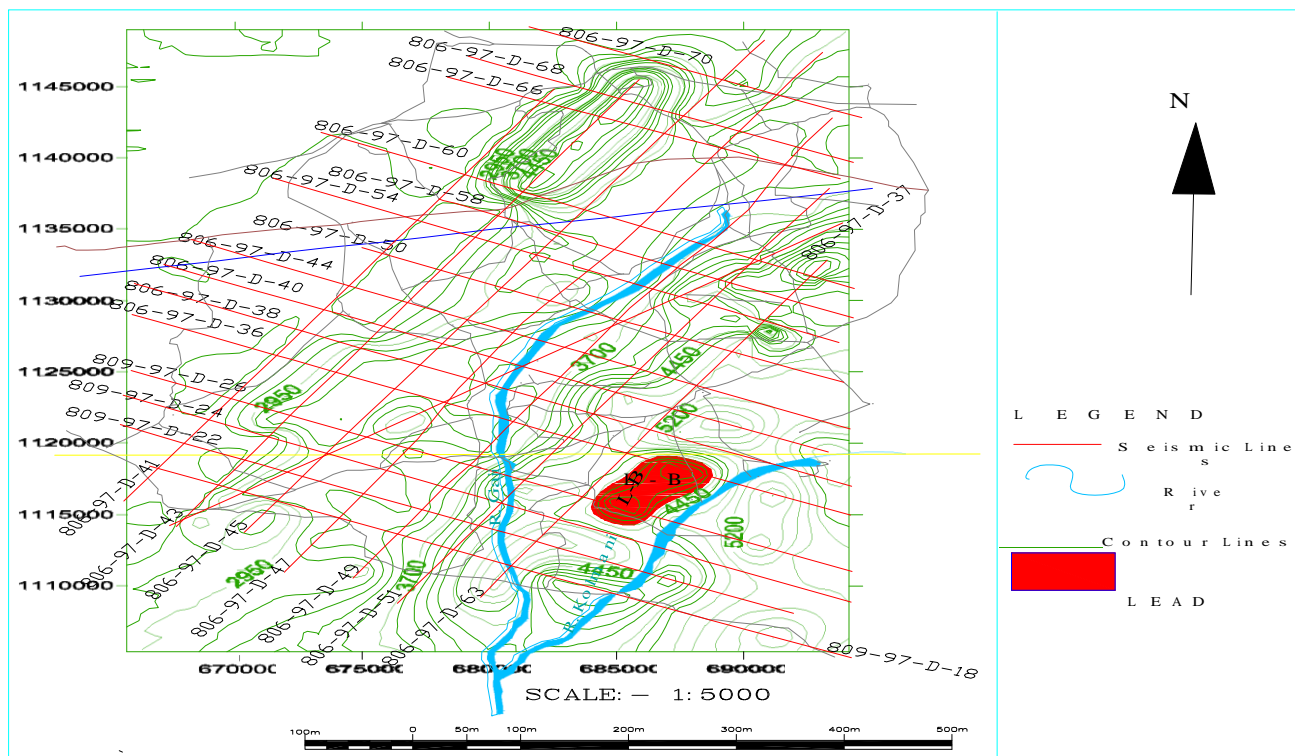**A8: Horizon H2 Depth Normalized Interval Velocity Map (contour interval =50m/s)**

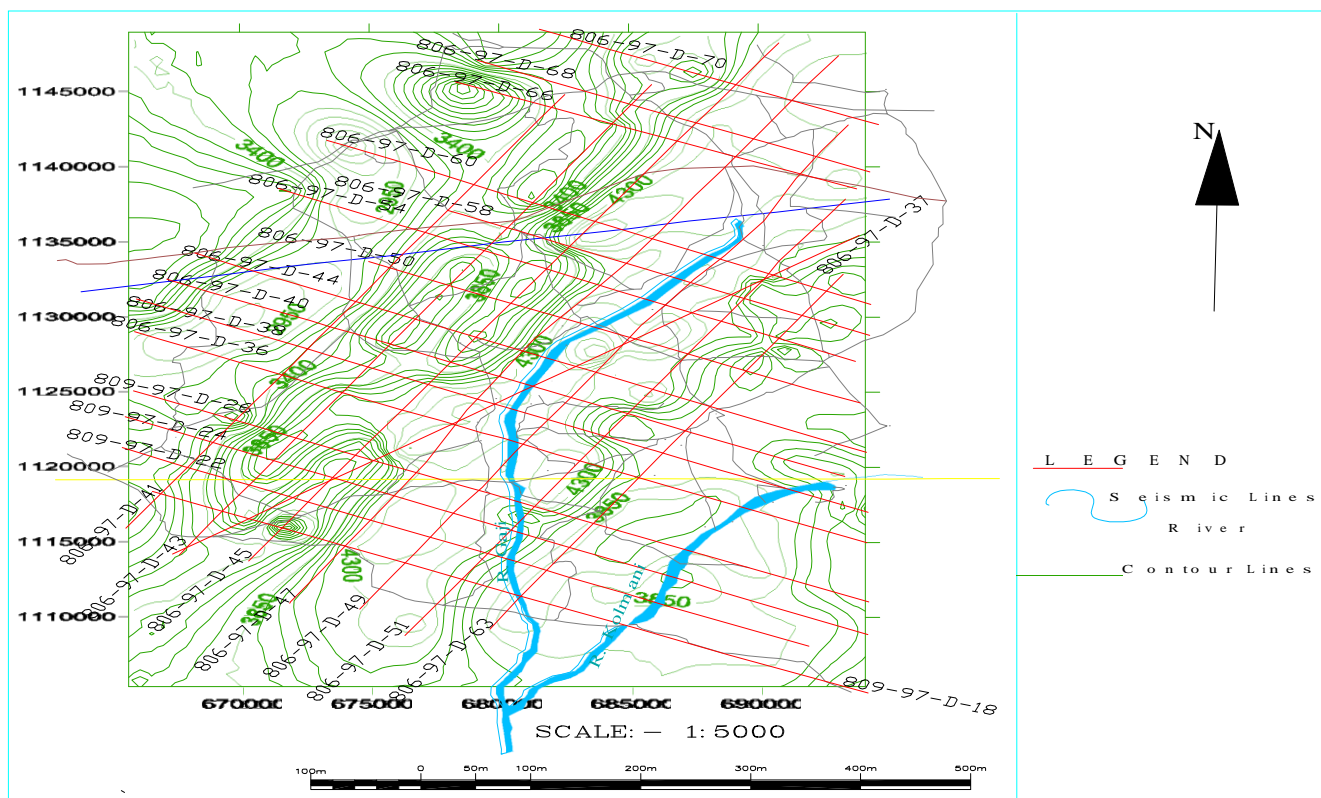**A9: Horizon H3 Depth Normalized Interval Velocity Map (contour interval =50m/s)**

A10: Horizon H5 Depth Normalized Interval Velocity

A11: **Horizon H6 Depth Normalized Interval Velocity Map**

A12: Top Basement Depth Normalized Interval Velocity Map

Acknowledgement
We thank Shell Nigeria Exploration and Production Company for the release of the data used in this research.

Bibliography
Al Chalabi, M., (1974), An Analysis of Stacking rms Average and Interval Velocities over a Horizontally Layered Ground, Gophys Prosp., v22, p458-475.

Avasthi, D. N and Verma, S. K (1973): Analysis of the Statistical Structure of Seismic Reflection for Delineation of Stratigraphic Traps for Oil, Symposium on Recent Trends in Exploration of Minerals, Oil and Ground Water, New Delhi, India

Avbordo, A A(1978): Geology and Hydrocarbon Productive Trends 0f Southern Nigeria Basin. The Oil and Gas Journal. Pg 90-93.

Badley, M. E, Anstey, N. A (1988) : Seismic Contouring GP 502. Exploration Geophysics

Beck, A. E (1981): Physical Principles of Exploration Methods. Macmillian Press Limited   London.

Bishop, T. N; Bube, K. P.; Cutler, R. T.;Langan, R. T.; Love, P. L.; Resnick, J. R.; Shuey, R. T.; Spindler, D. A. and Wyld, H. W. (1985). Tomographic determination of velocity and depth in laterally varying media; Geophysics50, 903-923.

Chen, C. U. (1978): Seismic Pattern Recognition, Geoexploration, Elservier, Amsterdam

Chiu, S. K; Kanasewich, E. R.; and Phadke, S. (1986). Three – dimensional determination of structure and velocity by seismic tomography: Geophysics, 51. 1559-1571.
Bhaskara Rao, D. (1990): Analysis of Gravity Anomalies of Sedimentary Basin By Trapezoidal Model

Coffen, J. A (1978): 3-D Field Work and Processing. Exploration geophysics GP 702/704

Dix, C. H., 1995, Seismic velocities from surface measurements: Geophysics, 20, 68-86.

Dobrin, M. B (1980): Geophysical Prospecting. McGrawhill Book Company, New York.

Dobrin, M. B (1977): Seismic Exploration for Stratigraphic Traps, in AAPG Memeoir no 26, Ed. C. E. Payton, 516p.

Gardner, G. H. F, Gardner, L. W. and Gregory, A. W. (1974):   Formation Velocity and Density- the Diagnostic Basis for Stratigraphic Traps, Geophysics, v39, p770-780.

Gardner, G.H.F., (1985), Migration of seismic data: Geophysics reprint series. No. 4: Soc. Expl. Geophys.

Gerristma, P.H. A., (1977), Time – to – depth conversion in the presence of structure: Geophysics, 42. 760-772.

Grant, F. S, West, G. F.(1987) Interpretation Theory In Applied Geophysics. McGrawhill Book Company, Toronto.

Hossack, J.R., (1979), The Use Of Balanced Cross – Sections In The Calculation Of Orogenic Contraction: A review: J. Geol. Soc. London, 136, 705-711.

Hron, P., 1977, Time migration – some ray theoretical aspects: Geophys. Props., 25. 738-745.

Keary, P and Brooks, M (2002). An Introduction to Geophysical Exploration . London.

Kennett, B. L and Harding, A. J. (1985). Is ray theory adequate for reflection seismic modeling? (a survey of modeling methods)

Levin, F. K.,(1971). Apparent Velocity From Dipping Interface Reflections: Geophysics, 36. 510-516.

May. B.T., and Covey, J.D., (1981). An Inverse Ray Method For Computing Geoloe Structures From Seismic Reflections – ero – offset case: Geophysics. 46, 268-287.

Melran, D. C, Siraki, E. S, Douglas, J. C (1993) Velocity Interpretation and Depth Conversion. Exploration Geophysics Series GP 504.

Nettleton, I. L. (1976): Gravity And Magnetics In Oil Prospeting. New York: Mcgraw Hill

Phil, Schultz (1998) the Seismic Velocity Model As An Interpretation Asset. Society Of Exploration Geophysics, Tulsa, USA.

Shah, P. M., (1973), Ray Tracing In Three Dimensions: Geophysics, 38, 600-604.

Sherrif, R. E (1975): Factors Affecting Seismic Amplitudes., Geophys Prosp, v23, p125-138.

Sherrif, R. E (1976): Inferring Stratigraphy from Seismic Data, Bull AAPG, v60, p528-542

Sherrif, R. E (1987): Seismic Stratigraphy . International Human Resources Development Corporation, Boston, USA.

Shuey, T. N., Bube, K.P., Culter, R. T. Langan, R.T., Love, P.L., Resnick, J.R., velocity and depth in laterally varying media: Geophysics, 50, 903-923.

Sinvhal, A ,Sinvhal, H (1992) Seismic Modeling and Pattern Recognition In Oil Exploration. Kluwer Academic Publisers, Netherland.

Skeen, P.M., (1983). Seismic Models And Interpretation Of The Caspar Arch Thrust: Application to Rocky Mountain foreland structure: in Lowell. J.D., Ed., Rocky
Mountain foreland busins and uplifts: Rocky Mountain Assn. Geologists, 99-124.

Taner, M. T.; Cook, E. E., and Neidell, N. S (1970) Limitations of the seismic reflection methods- Lessons from computer simulations: Geophysics, 35.551-573.

Telford, W.M, Geldart, C. P, Sheriff, R. T, Keys, D. A (1990): Applied Geophysics. Cambridge University Press.

Toby, D (2005). Well Logging and Formation Evaluations. Elsevier Inc. USA.

Turker, P. M, Yorston, H. H (1985): Pitfalls In Seismic Interpretation. Society of Exploration Geophysicist , Oklahoma.

Wason, C.B. Black, J. I., and King. G.A. (1984), Seismic Modeling And Inversion: Proe, Inst. Elect. Electron. Eng. 72. 1385-1393.